Will climate change drive 21st century burn rates in Canadian boreal forest outside of its natural variability: Collating global climate model experiments with sedimentary charcoal data

Suggested running head: Future burn rates in Canadian boreal forests

Yves Bergeron[1]
NSERC-UQAT-UQAM industrial Chair in sustainable forest management, Université du Québec en Abitibi-Témiscamingue, 445 boul. de l'Université, Rouyn-Noranda, QC, J9X 5E4, Canada

Dominic Cyr
Centre d'étude de la forêt, Université du Québec à Montréal, Succ. Centre-ville, C.P. 8888, Montréal, QC, H3C 3P8, Canada

Martin P. Girardin
Natural Resources Canada, Canadian Forest Service, Laurentian Forestry Centre, 1055 du P.E.P.S., P.O. Box 10380, Stn. Sainte-Foy, Québec, QC, G1V 4C7, Canada

Christopher Carcaillet
Centre for Bio-Archeology and Ecology (UMR5059 CNRS) & Paleoenvironments and Chronoecology (PALECO EPHE), Université Montpellier 2, 163 rue Broussonet, F-34090, Montpellier, France.

[1] Corresponding author: Yves.Bergeron@uqat.ca

Abstract. Natural ecosystems have developed within ranges of conditions that can serve as references for setting conservation targets or assessing the current ecological integrity of managed ecosystems. Because of their climate determinism, forest fires may be viewed as a major vulnerability process to climate change for forests. We evaluated future trends and rates of change in fire activity under climate change in the eastern Canadian boreal forest and investigated whether these changes were included in the variability observed during the Holocene. Prediction of future annual area burned was made using simulated Monthly Drought Code data collected from an ensemble of seven global climate models and four scenarios of radiative forcing. Past burn rates (7000 cal years BP to present) were inferred from sedimentary charcoal analyses from three lakes. The increase in burn rate that is predicted for the end of the 21st century (0.45% yr^{-1} with 95% confidence interval [0.32, 0.59]) falls well within the long-term variability (0.37 to 0.90% yr^{-1}) that was derived from the paleo-fire reconstruction. While our results suggest that the predicted change in burn rates *per se* will not move this ecosystem to new conditions not encountered in the past, the impacts of increasing fire incidence cumulated to current rates of clear-cutting or other low-retention types of harvesting, which still prevail in this region, remain preoccupying.

Introduction

Natural ecosystems have evolved within ranges of conditions that can serve as references for setting conservation targets or assessing the current ecological integrity of managed ecosystems (Landres *et al*. 1999). Disturbance regimes are key processes in many types of ecosystems and they contribute to a large extent to the creation of a variety of ecological conditions that exist through both space and time (Reynolds 2002). Disturbance regime characteristics, including frequency, spatial extent and severity, are particularly important in generating this natural variability at various spatial and temporal scales.

In this paper we focus on the influence of disturbance frequency, which can be expressed as the mean fire interval (MFI) or its opposite, that is, the percent annual burn rate (1/MFI; % yr^{-1}). When stand-replacing fires are predominant, which is the case in the continental regions of the boreal forest, the MFI is largely responsible for the creation of a complex landscape mosaic consisting of stands varying in age, composition and structure, within which other disturbances and processes interact (Wein and MacLean, 1983; Johnson 1992, Payette 1992, Niklasson and Granström 2000).

Reconstruction of fire history in western Quebec boreal forests for the last 7000 years is well documented (Bergeron *et al*. 2004; Cyr *et al.* 2009). The high variability observed during the Holocene, despite slight changes in vegetation composition (Carcaillet *et al.* 2001; Ali *et al*. 2008; Carcaillet *et al*. accepted), highlights the fact that the natural landscape mosaic has natural resilience to change in fire frequency.

Because of their climate determinism, forest fires may be viewed as a major process of vulnerability to climate change for forests (Le Goff *et al.* 2005; Flannigan *et*

67 *al.* 2009). Climate change may be defined as a change in the state of the climate that can
68 be identified by changes in the mean and/or variability of its properties and that persists
69 for an extended period of time, typically decades or longer. However, as in the United
70 Nations Framework Convention on Climate Change, we herein more specifically define
71 climate change as "a change of climate which is attributed directly or indirectly to human
72 activity that alters the composition of the global atmosphere and which is, in addition to
73 natural climate variability (e.g. solar, orbital forcing), observed over comparable time
74 periods" (United Nations 1992). Already, climate change has had a significant influence
75 on area burned in Canada. Forest fire activity has increased steadily over the second half
76 of the 20th century, (Podur *et al.* 2002, Stocks *et al.* 2003), and part of this rise has been
77 attributed to climate change (Gillett *et al.* 2004). Confounding influences may also have
78 added up, notably from changes in the atmospheric circulation patterns governing
79 regional fire activity (Macias-Fauria and Johnson 2006, Skinner *et al.* 2006,) or changes
80 in land use (Podur *et al.* 2002).

81 Climate change has direct and indirect impacts on forest ecosystems. Direct
82 impacts include the alteration of species growth, reproduction and migration while
83 indirect impacts correspond to modifications of disturbance regimes such as forest fires,
84 insect outbreaks and diseases (Dale *et al.* 2001). Indirect impacts, such as changes in fire
85 regimes, may have more dramatic results than direct impacts, which take a long time to
86 materialize (Overpeck *et al*. 1990; Weber and Flannigan 1997).

87 The objective of this paper was to evaluate future trends and rates of change in
88 fire activity under climate change in eastern Canadian boreal forests and determine
89 whether these changes were included in the observed variability during the Holocene.

First, we used regression analyses to model the historical (1959–1999) relationship between climate and area burned by large forest fires (size >200 ha). These models were then used as transfer functions for predictions of future area burned. This was done by substituting historical climate conditions by future one simulated from an ensemble of seven global climate model (GCM) experiments driven by four scenarios of radiative forcing. These predictions were used to generate changes in burn rate between three reference periods: 1959–1999, 2046–2065 and 2081–2100. Next, we compared these predicted changes to Holocene MFI as reconstructed by sedimentary charcoal analyses from three lakes (Cyr *et al*. 2009). Finally, we discuss implications of predicted future fire activity in the context of the natural range of variability observed during the Holocene.

Study area

The study area (Fig. 1) is located in the boreal zone of western Quebec and eastern Ontario (Canada). This part of the Precambrian Shield is covered with glacio-lacustrine clays that have been reworked by glacial surges, resulting in a relatively compact deposit composed of clay and gravel that is called the Cochrane Till (Veillette 1994). The mostly flat region (mean altitude ~250 m a.s.l.) shows three major soil types, Luvisols, Gleysols and Organic Soils (Soil Classification Working Group 1998), which reflect the variable thickness of the organic layer (about 10 to > 200 cm). The dominant forest types are black spruce (*Picea mariana* (Mill.) B.S.P.) - feathermoss and black spruce - *Sphagnum*, with an understory dominated by ericaceous shrubs (*Rhododendron groenlandicum*, *Kalmia angustifolia*, *Vaccinium* spp). Jack pine (*Pinus banksiana* Lamb.) and trembling

aspen (*Populus tremuloides* Michx.) also occur in pure or mixed stands, and secondary tree species include balsam fir (*Abies balsamea* (L.) Mill.), paper birch (*Betula papyrifera* Marsh.), and tamarack (*Larix laricina* (DuRoi) K. Koch) (Gauthier *et al.* 2000). The region's mean annual temperature is –0.7°C (mean temperatures for January and July are –20.0°C and 16.1°C, respectively), and annual precipitation is 905 mm, 35% of which falls during the growing season (Matagami weather station [49°46'N, 77°49'W], Environment Canada 2006).

Data and methods

Present-day fire data

Forest fire data from the large fire database (LFDB, Stocks *et al.* 2003) are used in this study to develop the predictive model for annual area burned. These large fires (size >200 ha) represent only a very small percentage of fires but account for ~97% of the area burned in Canada. The LFDB contains information on start location, estimated ignition date, cause and size of each fire. Fires that occurred within the territory defined as 83°W to 75°W and 47°N to 53°N were compiled (Fig. 1) and a time series of annual area burned covering the period 1959–1999 was created. Fire is highly variable among years and the use of a large number of samples provided some statistical smoothing that improved the final calibration results and minimized the prediction error. This territory of 32.9 M ha was therefore found to offer the best compromise between selecting a region with a disturbance regime representative enough of the surroundings of the sampled lakes and maximizing the signal-to-noise ratio in the fire dataset. Although they don't apply to the exact same periods, the recent burn rates estimated for the 32.9 M ha territory from

136 the LFDB during the 1959-1999 period was 0.24% per year while it was estimated to
137 0.27% during the 1920-1998 period for a smaller area located in the surroundings of the
138 sampled lakes from a dendroecological study (Bergeron et al. 2004).
139
140 *Predictors of future fire conditions*
141 The predictors of area burned used in this study included monthly means of daily mean
142 temperatures and the monthly Drought Code (hereafter called MDC), an index
143 representing the net effect of changes in evapotranspiration and precipitation on
144 cumulative moisture depletion in deep, compact organic layers (Girardin and Wotton
145 2009). The MDC was previously shown to be a robust predictor of area burned across
146 circumboreal forests (Girardin *et al.* 2009a). Monthly mean temperatures also proved to
147 be a robust predictor of area burned across North American boreal forests (Balshi *et al.*
148 2009), and therefore it is used in our model calibration.
149 The MDC is a generalized monthly version of the daily Drought Code widely
150 used across Canada by forest fire management agencies in their monitoring of wildfire
151 risk. The MDC was developed by Girardin and Wotton (2009) to be used in seasonal
152 drought characterization analyses when the daily weather data necessary for computation
153 of the daily Drought Code are not available.
154 The Drought Code represents the moisture content of organic matter that is on
155 average about 18 cm thick and 25 $kg \cdot m^{-2}$ dry weight, for a bulk density of 138.9 $kg \cdot m^{-3}$.
156 The equation linking the Drought Code (DC) to its moisture equivalent (Q; unitless) is:
157 $$Q = 800 \cdot e^{-DC/400} \qquad [1]$$

158 The 400 constant in Eq. 1 represents the maximum theoretical moisture content of the
159 fuel represented by the Drought Code, which roughly corresponds to the water-holding
160 capacity of the soil, i.e. 100 mm (Van Wagner 1987). In its daily version, the Drought
161 Code has a response time of 62 days at 15°C and 44 days at 30°C. This long response
162 time served as the basis for the development of a monthly approximation model.

163 The MDC formulation may be summarized as follows. First, potential
164 evapotranspiration E (unitless quantity) over month m follows the method of
165 Thornthwaite and Mather (1955) and is given by:

166 $$E_m = N \cdot (0.36(\overline{T}_{mx}) + L_f) \qquad [2]$$

167 where $\overline{T}_{mx}$ is the monthly mean of daily maximum temperatures (°C), L_f is the standard
168 day length adjustment factor (Van Wagner, 1987), and N is the number of days in the
169 month. Next, computation of the MDC is carried out twice in a month to reduce bias that
170 may arise when the forest floor becomes saturated in the spring. Drying taking place over
171 the first half of the month (DC_{HALF}) is calculated as:

172 $$DC_{HALF} = MDC_0 + 0.25E_m \qquad [3]$$

173 where MDC_0 is the MDC from the end of the previous month. Total monthly rainfall (r_m)
174 is simulated to occur in the middle of the month, and the moisture equivalent in the layer
175 after rain Q_{mr} (unitless) is calculated as:

176 $$Q_{mr} = 800 \cdot e^{(-DC_{HALF}/400)} + 3.937 \cdot RM_{EFF}. \qquad [4]$$

177 In these equations, r_m is reduced to an effective rainfall (RM_{EFF}; mm) after canopy and
178 surface fuel interception using $RM_{EFF} = 0.83 \cdot r_m$. An estimate of the MDC value at the
179 end of the month (MDC_m; unitless), for which total rainfall and mean temperature apply,
180 is calculated as:

$$MDC_m = 400 \cdot \ln(800 / Q_{mr}) + 0.25E_m . \qquad [5]$$

Finally, MDC_0 and MDC_m are averaged to find a mean drought value for the month:

$$MDC = (MDC_0 + MDC_m) / 2 . \qquad [6]$$

When calculating the next month's MDC, the value of MDC_m from the previous month then becomes the new MDC_0.

Girardin and Wotton (2009) found that the MDC generally followed trends in the monthly means of the daily Drought Code closely (r^2 ranging from 0.87 to 0.95 for n = 612 sample months). There are no absolute guidelines as to the meaning of MDC values but, generally speaking, Drought Code values below 200 are considered low while values around 300 may be considered moderate in most parts of the country. A Drought Code rating of 400 or more indicates that fire could involve burning of deep sub-surface and heavy fuels (e.g. de Groot *et al.* 2009). The index generally peaks in mid- to late August, beyond which it either declines or maintains the same value; during extreme years with late season fires, this does not always hold true (McAlpine 1990; Girardin *et al.* 2004). The reversal in August is only attributed to a change in day length, and is not a function of seasonal precipitation.

Climatic data

Monthly means of daily mean and maximum temperatures and monthly precipitation totals were obtained for the 1959–1999 period using BioSIM (Régnière and Bolstad 1994). Data were obtained for 100 locations distributed across 83°W to 75°W and 47°N to 53°N by interpolating data from the four closest weather stations to each location, and adjusting for differences in latitude, longitude and elevation between the data sources and

each of the locations. The MDC and mean monthly temperatures were computed at each location and data were then averaged to create regional mean monthly data. In order to give greatest weight to climate anomalies in fire-prone regions (Gillett *et al.* 2004; Girardin and Wotton 2009), the distribution of locations was made such that regions having higher fire frequencies also had higher location replicates (see Fig. 1).

Prediction of future annual area burned is made using simulated monthly temperature and precipitation data collected from an ensemble of seven GCMs (Table 1). Model selection was made accordingly with the availability of monthly means of daily maximum temperature outputs necessary for simulation of MDC. GCMs are time-dependent numerical representations of the atmosphere and its phenomena over the entire planet, using the equations of motion and including radiation, photochemistry, and the transfer of heat, water vapour, and momentum. Future climate scenarios are built based on the effects of various concentrations of greenhouse gases and other pollutants within the atmosphere on the earth-atmosphere system. Monthly temperature and precipitation data were collected from four to six cells (depending on model resolution) located near the region, and averaged. Data were collected for horizons 1961–1999, 2046–2065 and 2081–2100.

GCMs can have large biases when it comes to reproducing the regional features of climate. To account for differences between the actual climate data derived from BioSIM and the GCM predictions, we adjusted the monthly simulations relative to the absolute difference from the 1961–1999 monthly means of actual data (e.g. Balshi *et al.* 2009). A correction was also applied to the interannual variability by changing the width of the distributions so that mean monthly GCM predictions and data derived from BioSIM had

equal standard deviations over their common period 1961–1999 (Girardin and Mudelsee 2008). The following algorithm was used in doing these corrections:

$$GCM_{adj} = BioSIM\mu + (GCM_{month} - GCM\mu) \cdot \delta, \qquad [7]$$

where GCM_{adj} is the corrected monthly value output of the GCM predictions, $BioSIM\mu$ is the mean monthly value (across all years) for the period 1961–1999 derived from BioSIM, GCM_{month} is the monthly value output by GCM predictions, $GCM\mu$ is the mean monthly value (across all years) for the period 1961–1999 derived from the GCM monthly predictions, and δ is the ratio of the standard deviation in monthly values (across all years) for the period 1961–1999 derived from BioSIM compared to that derived from GCM monthly predictions ($\delta = BioSIM\sigma / GCM\sigma$). This ratio inflates or deflates the simulated interannual variations.

Four scenarios of projected changes in greenhouse gas emissions (Nakicenovic *et al.* 2000) are used in this study (from "worst" to "best" case scenarios): A2, A1B, B2 and B1. Each scenario reflects a specific storyline of future development such as global population growth, economic development, and technological change. The storylines describe the relationships between the forces driving greenhouse gas and aerosol emissions and their trajectories over the 21st century (http://sedac.ciesin.org/ddc/sres/index.html):

- A2 storyline (intense forcing): a very heterogeneous world with continuously increasing global population and regionally-oriented economic growth that is more fragmented and slower than in other storylines.

- A1B storyline (intense forcing): a future world of very rapid economic growth, global population that peaks in mid-century and declines thereafter, and rapid introduction of new and more efficient technologies with low carbon emissions.
- B2 storyline (intermediate forcing): a world in which the emphasis is on local solutions to economic, social and environmental sustainability, with continuously increasing population (lower than A2) and intermediate economic development.
- B1 storyline (intermediate forcing): a convergent world with the same global population as in the A1B storyline but with rapid changes in economic structures toward a service and information economy, with reductions in material intensity, and the introduction of clean and resource-efficient technologies.

These storylines are intended to cover a wide spectrum of alternative futures to reflect relevant uncertainties and knowledge gaps associated with climate change issues (Nakicenovic *et al.* 2000).

Predictive model for area burned

Development of a predictive model for area burned is carried out using Multivariate Adaptive Regression Splines (MARS) (Friedman 1991). MARS is a technique in which non-linear relationships between a predictand (i.e. variable to predict) and a predictor are described by a series of linear segments of differing slopes, each of which is fitted using a basis function. Breaks between segments were defined by an inflection point in a model that initially over-fitted the data, and was then simplified using a backward/forward stepwise cross-validation procedure to identify terms to be retained. At each step, the model selected the inflection point and its corresponding pair of basis functions that gave

271 the greatest decrease in the residual sum of squares. Selection was proceeded until some
272 maximum model size was reached, after which a backward-pruning procedure was
273 applied in which those basis functions that contributed least to model fit were
274 progressively removed. The sequence of models generated from this process was then
275 evaluated using generalized cross-validation, and the model with the best predictive fit
276 was selected. For the present study, annual area burned was regressed against the MDC
277 and mean temperatures from April to October over the 1959–1999 period (total of 14
278 potential predictor variables). Once the model is developed, it may then be used as a
279 transfer function for prediction of future area burned. This is done by substituting
280 historical climate conditions by future ones generated from the GCM experiments. For
281 other applications of MARS, see Leathwick *et al.* (2005), Balshi *et al.* (2009), and
282 Girardin *et al.* (2009b). The R package 'earth', specifically designed for MARS using the
283 techniques described by Friedman (1991), was used for calibration of model parameters
284 (R Development Core Team 2007). The Generalized Cross Validation (GCV) penalty per
285 knot was set to two. Other parameters were kept as in the 'earth' default settings.
286
287 *Paleoecological reconstruction of MFI and natural range of variability*
288 A long-term fire history was reconstructed using sedimentary charcoal from three lakes
289 and dated using ^{14}C and ^{210}PB isotopes (Carcaillet *et al.* 2001, accepted). These three
290 lakes were considered as representative of the study area. Only charcoal fragments larger
291 than 150 µm were considered as particles of this size generally do not travel more than a
292 few hundreds of meters from a fire (Higuera *et al*. 2007). Charcoal accumulation peaks
293 were then isolated to build fire event chronologies beginning as far back as 7600 cal. yr

294 BP for one of the lakes, although only results spanning the last 6800 years were available
295 for all three lakes (see method in Carcaillet *et al*. 2001). The fire intervals from the three
296 lakes were pooled to estimate the mean fire interval (MFI) across the landscape, which
297 we define as the average number of years between two successive fire events at a given
298 point (cf Merrill and Alexander 1987). We assumed that the ratio between the charcoal
299 source-area and the typical size of fires in this area is negligible and, therefore, we
300 considered these lakes as a point-based representation of fire activity. About 80% of the
301 total area burned between 1959-1999 was indeed affected by individual fires larger than
302 8500 ha and charcoal source-area represented by these lakes was most likely between
303 several tens and a few hundred hectares (Higuera *et al*. 2007). Li (2002) demonstrated
304 that the derivation of point-based estimates of fire activity such as the MFI to obtain an
305 area-based one is possible when the sampled sites are independent of each other and if the
306 observations cover a period of several times the MFI. Both conditions are met as our
307 paleoecological fire history reconstruction cover 6800 years and as the nearest lakes are
308 located 56 km from one another. A similar paleoecological reconstruction conducted
309 nearby from sedimentary charcoal also shows an asynchrony of recorded fire events in
310 lakes that are actually closer to one another (Ali *et al* 2009). Our estimations of MFI were
311 then reversed to obtain estimations of average burn rates (burn rate = 1/MFI ; cf Li 2002).
312 To assess the long-term natural variability in MFI (and burn rate), we first
313 estimated MFI within periods of relatively constant regimes using the two-parameter
314 Weibull probability density distribution fitted over the observed fire intervals (not shown,
315 see Carcaillet *et al.* 2001 or Cyr *et al.* 2009). The Weibull-modeled MFI during these
316 periods were used to define a first range of long-term natural variability that will be

317 referred to as the **conservative range,** which is suggested as a management guideline by
318 Cyr *et al*. (2009), while the corresponding 95% confidence intervals were used to define
319 an **extended range** of natural variability. The second approach was a smoothing method,
320 which we used to fit the Weibull distribution within a moving window of 13 observations
321 and report the estimated MFI along our time series. This moving window roughly
322 corresponded to a little more than 1000 years during periods with low fire frequency and
323 about 300 years during periods with high fire frequency. The smoothing method shows
324 shorter term variations which are reported for comparative purposes.
325
326 **Results**
327 *Climate simulations*
328 Simulations from the seven GCMs showed agreement as to the direction of future
329 temperature changes in our study area, regardless of radiative forcing scenarios (Fig. 2).
330 Warming is expected to occur throughout all months of the year, with winter months
331 showing the greatest rates of change. By the end of the 21st century, daily maximum
332 temperatures during summer months are predicted to be warmer by about 4°C when
333 compared to 1961–1999.
334 The rate of change in precipitation predicted from the ensemble of GCMs is not as
335 univocal as the one in temperature. About half of the simulations predicted a decrease in
336 summer precipitation (down by 18% when comparing 1961–1999 with 2081–2100
337 horizons), while an increase in precipitation was predicted by the other half (up by 11%).
338 An increase in precipitation is predicted for fall, winter and spring months by all models
339 (from 8% to 41% in spring and from −1% to 20% in fall).

340 The influence of climate on forest fire involves a trade-off between the amount of
341 precipitation and temperature. Our estimates of the net effects of changes in
342 evapotranspiration and precipitation on cumulative moisture depletion in soils suggest
343 that the uncertainty in modelled precipitation changes will be exacerbated by the large
344 increases in temperature. In 17 out of 19 of our simulations (i.e. 90% of our simulations),
345 MDC was predicted to increase by the end of the 21st century, resulting in an increase
346 median ensemble MDC in all months from April to October (Fig. 3). In the few cases
347 where the MDC was predicted to decrease (particularly during the mid-century), the
348 emission scenario was forced by a B1 storyline of low population growth with rapid
349 technological changes (intermediate forcing). It is noteworthy to mention that in spite of
350 this general agreement with regard to the direction of summer moisture changes,
351 uncertainty remains important as suggested by the 10th and 90th percentiles, up to 80
352 MDC units for August (Fig. 3).
353
354 *Predictive model for area burned*
355 We regressed the annual area burned (AAB) against the MDC and mean temperatures
356 over 1959–1999 using MARS. The regression model explained 42% of the deviation
357 between the variable to predict and the predictors ($P < 0.001$; GCV-$R^2 = 0.36$) and took
358 on the following form:

359
$$\begin{aligned} BF_1 &= \max(0, MDC_{August} - 192.36) \\ AAB &= 8490.7 + 2201.0 * BF_1 \end{aligned} \quad . \quad [8]$$

360 where MDC_{August} is the August MDC. The calibration error in AAB estimates was
361 0.061 M ha per year. In the MARS model, the inflection point for the MDC variable takes
362 on a value of 192.36, and the basis function (BF_1) takes on a value of MDC minus 192.36

363 when MDC is >192.36, but otherwise takes on a value of zero (Fig. 4). Coefficients
364 applied to the basis function define the slopes of the non-zero sections. Dividing the
365 calibration interval (see Girardin and Mudelsee 2008) led to partial changes in the
366 relationship. Specifically, July MDC showed up as a potential AAB predictor depending
367 on period divisions. However, the July MDC was discarded as it is highly collinear with
368 the August MDC (Pearson $r = 0.89$, $P < 0.001$). Monthly means of daily mean
369 temperature did not show a significant relationship with AAB.
370
371 *Simulation of future burn rates*
372 Predicted changes in burn rates from the ensemble of seven GCMs forced by various
373 scenarios of greenhouse gas emissions are shown in Figure 5. A wide array of
374 model/scenario outcomes suggests a fairly large amount of uncertainty in predictions of
375 future burn rates. Simulations from the Canadian and the National Institute for
376 Environmental Studies GCMs (i.e. CGCM3T63 and MIROC3.2 medres) yielded the
377 greatest rates of change. For instance, the CGCM3 A2 simulation suggested a change in
378 burn rate from a current value of 0.24% yr^{-1} to one of 0.69% yr^{-1} for the end of the 21st
379 century. Other models, like the GISSAOM, suggested moderate changes in burn rate in
380 the course of the 21st century. All models suggested that the future burn rate will remain
381 below 1.00% yr^{-1}.
382 Modelling uncertainty was dealt with by randomizing of the AAB simulations
383 using a bootstrap method and recomputing the burn rate for each horizon using the 2.5%,
384 50%, and 97.5% AAB percentiles. This yielded an 'ensemble-mean' burn rate and a 95%
385 confidence interval (CI) for each horizon (Fig. 5). Not only does this 'uncertainty band'

386 take into account climate modelling and greenhouse gas emissions uncertainties, but it
387 may also partly take into account errors owed to various assumptions in our data and the
388 calibration error (a calibration error of 0.061 M ha per year corresponds to an error in the
389 estimated burn rate of ±0.18% yr^{-1}). Burn rates for ensemble-mean scenarios A2, A1B
390 and B1 were also computed (Table 2). However, one should note that ensemble-mean
391 scenarios were obtained from limited GCM experiments (six GCM experiments per
392 scenario), which may explain the wide uncertainty bands. The ensemble mean of all 19
393 simulations suggests an increase in the burn rate of our study area from a current value of
394 0.20% yr^{-1} (95% CI [0.12, 0.28]) to 0.36% yr^{-1} (95% CI [0.25, 0.48]) by the mid-21st
395 century, and 0.45% yr^{-1} (95% CI [0.32, 0.59]) by the end of the 21st century. Upper and
396 lower bounds of this ensemble-mean CI (Fig. 5) closely approximate burn rates
397 calculated from ensemble-mean scenarios A2 and B2, respectively (Table 2). Will these
398 values be within the historical variability?
399
400 *Past natural variability* vs *predicted burn rate*
401 The period between 6800 and 3200 cal. yr BP was characterized by a relatively low burn
402 rate, while the period after 3200 cal. yr BP shows a considerable increase with a
403 subsequent decrease during the last millennium (Fig. 6). Climatic drivers are currently the
404 most plausible explanation for these changes, as pollen records show no relationships
405 between vegetation, based on pollen composition and diversity, and fire activity during
406 this period (Carcaillet *et al.* 2001), both in terms of trends and timing of paleo-fire and –
407 vegetation modification (Carcaillet *et al*. accepted). Using these periods of relatively
408 constant regimes, the conservative range of variability in burn rate varies between 0.37%

409 yr^{-1} (MFI ≈ 267 years) and 0.90% yr^{-1} (MFI ≈ 111 years), while the extended range varies
410 between 0.24% (MFI ≈ 419 years) and 1.22% yr^{-1} (MFI ≈ 82 years) (Cyr *et al*. 2009). The
411 smoothing method shows shorter-term variations, which are generally encompassed by
412 the extended range of natural variability.
413 The increase in burn rate that is predicted by the end of the 21st century, +0.45%
414 yr^{-1} (95% CI [0.32, 0.59]), falls within the long-term variability that was derived from the
415 paleo-ecological reconstruction. This predicted burn rate, which corresponds to a MFI of
416 222 years, is relatively low when compared with periods of higher burn rates, i.e.
417 between 3300 and 900 cal. yr BP, when the burn rate was oscillating at around a little less
418 than 1%. Moreover, the 95% confidence interval associated with the predicted burn rate
419 (corresponding to a range of MFI varying between 169 and 313 years) is also well
420 contained and quite smaller than the conservative and extended ranges of natural
421 variability.
422
423 **Discussion**
424 *Predicted increases in burn rate and critical assessment of the model*
425 This study used an ensemble-mean of 19 GCM experiments for prediction of future burn
426 rates in eastern Canadian boreal forests. These experiments investigate the effects of
427 different, but equally plausible, initial atmospheric and oceanic conditions and CO_2
428 forcing scenarios, on climate and fire behaviour (Intergovernmental Panel on Climate
429 Change 2007). Individual GCM experiments provide indications of the magnitude of the
430 natural variability in the system. This variability is the main cause for the large
431 uncertainty in GCM experiments under a given CO_2 scenario (see confidence intervals in

Table 2). On the other hand, the ensemble-mean allows distinguishing the approximate climate change signal from the natural variability. The ensemble mean allows the identification of the impact response of burn rate to the climate change signal. The only other study of future fire activity in boreal forests that we are aware of in which an ensemble-mean of GCM experiments was used is that of Scholze et al. (2006).

The main result of our study is that, whatever the CO_2 emission scenarios or the GCM used, the future burn rate is predicted to remain within the natural range of variability for this region of the boreal forest. Predicted burn rates by the ensemble-mean of all 19 GCM experiments (Fig. 5) and by individual ensemble-mean scenarios (Table 2) are lower than assessed by sedimentary charcoal data during the Holocene period. Even under the most extreme experiment of MIROC3.2medres A2, a 0.8% yr^{-1} burn rate (equivalent to a MFI of 125 years) was still found to be slightly below what was observed between 3300 and 900 cal. yr BP (Fig. 6; see also Cyr *et al*. 2009).

Our assessment is based on long-term variability in burn rate reconstructed from sedimentary charcoal data. The plausibility of the obtained results rests on the validity of two principal assumptions. One is that forest fire distribution be relatively homogeneous in the study area and across time, such that locations of the selected lakes be representative for the whole study area. Second, MFI is estimated from peaks in charcoal sediments originating from local source area around the lakes. However, present forest fire distribution is not homogeneous in the study area (see Fig. 1), and this for number of factors including variability in land-use and in fire detection and suppression (Lefort *et al.* 2003). Also, charcoal source area may sometimes be undefined; there is always a probability with charcoal sediments record that fire events originating from large and

455 distant fires be detected as small local fires (Higuera *et al.* 2007). Such uncertainty may
456 be taken into account by construction of confidence intervals (Fig. 6) that may encompass
457 some range of sampling errors.

458 To increase confidence, results may also be supplemented by other reconstruction
459 methods of past fire activity. Past fire activity in this part of the boreal forest has been
460 well documented with time-since-fire distributions reconstructed from
461 dendrochronological dating of forest stands and fire scars (Bergeron *et al*. 2004, 2006).
462 Consistent with our results from the charcoal sediments record, reconstruction of burn
463 rates for the last 300 years for a territory covering 15,000km^2 (Bergeron *et al*. 2004)
464 reports variations in burn rate that encompass the entire array of predicted burn rates for
465 2100 AD (Fig. 5; Table 2). The 0.8% yr^{-1} burn rate predicted for 2100 AD associated
466 with the most extreme experiment (MIROC3.2medres A2) is indeed lower than what was
467 observed during the Little Ice Age (prior to 1850 AD), where the burn rate was the
468 highest recorded in recent history, at around 1.09% (equivalent to a MFI of 92 years)
469 Girardin and Mudelsee (2008) in their analysis of late Holocene fire risk variability
470 inferred from tree-ring records collated to GCM modelling, also came to a similar
471 conclusion. Their results suggest probabilities of having future levels of extreme fire risk
472 conditions be within the historical range.

473 The conclusions drawn from this work should also be limited to the impact of
474 late-spring and summer climate variability on forest fire activity. Factors that are not
475 directly taken into account in the seasonal drought severity component could modulate
476 the projected increase in burn rates over the 21st century and could distort the predicted
477 trend. Effects of forest composition (coniferous *vs*. hardwood) and age structure on fuel

478 availability and moisture regimes, which are important determinants of fire activity under
479 a given climate (Hély *et al*. 2001), are not taken into account in the current simulations.
480 These limitations also apply to the work done by Flannigan *et al.* (2005), Bergeron *et al.*
481 (2006), Girardin and Mudelsee (2008), and Balshi *et al*. (2009). Changes in fire regimes
482 could lead to shifts in vegetation composition and structure that could provide feedback
483 to fire activity. However, such a feedback doesn't appear to be important in the region as
484 no significant or delayed impact on the pollen-inferred vegetation was detected in relation
485 with the variation in burn rate that was observed during the last 7000 years (Carcaillet et
486 al accepted; cf section below for additional details). Furthermore the dominance of black
487 spruce and a thick organic layer could very likely limit rapid changes in vegetation
488 composition (Lecomte *et al.* 2006). Other factors not considered by the predictive model
489 that may be of importance include changes in the frequency of small precipitation events
490 and their impacts on fine fuels, and changes in wind velocity and their impacts on fire
491 behaviour (Li *et al*. 2000). That being said, these variables are currently not important
492 predictors of area burned in the study area (Balshi *et al*. 2009, their grid points 80.0°W,
493 50.0°N and 80.0°W, 52.5°N presented in their Table A1). Other factors that were not
494 taken into account in this study include changes in ignition agents (lightning frequency
495 and human-caused ignition; Price and Rind 1994; Wotton *et al*. 2003), changes in land
496 use (e.g., fragmentation of landscapes), interactions with other natural disturbance agents
497 such as insect outbreaks and diseases, feedback to the climate system through increases in
498 trace gas emissions (Gillett *et al*. 2004), and alteration of surface energy exchanges
499 (Chambers and Chapin 2002). Simulations of future fire conditions using dynamic
500 climate-vegetation models (de Groot *et al.* 2003, Keane *et al*. 2004) would be relevant

501 when attempting to account for changes in lightning probability, vegetation and fuel types
502 under a changing climate regime.
503
504 *Stability and resilience of the ecosystem facing predicted increases in burn rate*
505 Despite major changes in burn rate, pollen-inferred vegetation reconstructions
506 were unable to report clear concurrent shifts in the regional vegetation linked to fire
507 during the last seven millennia (Carcaillet *et al*. 2001; accepted). These studies suggest
508 that vegetation is rather well adapted to fluctuations in fire activity, although some
509 species might locally have behaved individually (Ali *et al*. 2008). The stability of
510 available pollen records is particularly strong in black spruce-dominated areas (see also
511 eastward, Garralla and Gajewski 1992), a species that can cope well with the range of
512 fire-free intervals occurring under natural conditions. Its seeds stored in serotinous cones
513 allow for quick regeneration following fire, while its shade tolerance and layering
514 capacity allow for its persistence in the landscape without fire (Lecomte and Bergeron
515 2005). Although less abundant, both early successional species, such as jack pine and
516 aspen, and late successional species, such as balsam fir or white spruce, are currently
517 present in the forest mosaic (Gauthier *et al.* 2000). This emphasizes the possibility that
518 the burn rate was never sufficiently high or low to totally exclude them from the
519 landscape, although locally significant effects are observed on balsam fir (*Abies*
520 *balsamea*) that is closed to its natural range limit (Ali *et al*. 2008). Minor changes in
521 species' relative abundances or in the forest age structure could therefore occur with
522 expected changes in burn rates, but available pollen records suggest that these changes
523 are unlikely to cause a major shift towards an alternative state.

524 Moreover, the considerable variations in burn rate that were observed during the
525 last 300 years (Bergeron et al. 2004; Girardin and Mudelsee 2008) show that the rate of
526 change can be quite high under natural conditions. This observation suggests that systems
527 should be able to cope with the predicted change in the burn rate of +0.2% during the
528 next century (ensemble-mean of all 19 GCM experiments, Fig. 5).
529
530 *Management implications*
531 Fire activity is already an important issue for public safety and timber protection
532 (Martell 1994). The expected doubling of the burn rate for 2100 will have very significant
533 economical and social consequences that will require important adaptive measures.
534 Adaptive measures suggested previously include increased fire suppression efforts, fuel
535 management, salvage logging, regeneration enhancement, functional zoning and risk
536 assessments that are considered *a priori* in general strategic planning and annual
537 allowable cut (AAC) calculations (Le Goff *et al*. 2005 and other references therein).
538 Independently of the implementation and success of all these measures, the maintenance
539 of ecosystem resilience is a prerequisite to the sustainable management of the boreal
540 forest as it prevents the system from shifting towards an undesirable alternative state and
541 thus reduces uncertainty.
542 Forest ecosystem management, an approach that is gaining in popularity and that
543 aims to decrease the difference between managed and natural forests (Gauthier *et al*.
544 2009) by emulating natural disturbances through harvesting, may provide additional
545 solutions (see also Harvey *et al*. 2002, Kuuluvainen 2002, Attiwil 1994, Angelstam
546 1998). The rationale for such an approach is that fire is perhaps the most important

547 determinant of landscape compositions and stand structures and that maintaining these
548 through forest ecosystem management practices should in turn allow us to maintain
549 biological diversity, essential ecological functions and ecosystem resilience. As burn
550 rates get closer to the upper boundaries of the natural range of variability, it decreases the
551 necessary "room for manoeuvre" that allows the substitution of fire for harvesting as a
552 high-severity disturbance, hence limiting the extent to which we can emulate fire
553 (Bergeron *et al*. 2006). To maintain a comparable AAC while limiting the cumulative
554 impacts of these two stand-initiating disturbances (fire and clear-cutting), which together
555 are driving the system out of its natural range of variability (Cyr *et al*. 2009), we suggest
556 to increase the relative importance of uneven-aged management, which can be designed
557 to emulate finer-scale disturbances or individual mortality within stands. First, uneven-
558 aged management would contribute to maintaining old forest attributes in a landscape
559 where they were naturally and historically dominant. Second, it would contribute to
560 preventing the additional costs of regeneration failures that occur more frequently when
561 high-severity disturbances such as clear-cutting, fire and insect outbreaks happen within
562 short intervals of time (Jasinski and Payette 2005), a phenomenon that is likely to
563 increase as the pressure from low-retention harvesting and fire does.
564
565 *Conclusion*
566
567
568

569 Our results support precedent studies reporting that climate change will cause an
570 increase in burn rate over this part of the boreal forest (Flannigan et al. 2005, Girardin
571 and Mudelsee 2008). The increase in burn rate that we predict, from the present value of
572 0.20% yr^{-1} to 0.45% yr^{-1} with 95% confidence interval [0.32%, 0.59%] by the end of the
573 21st century, might appears important at first but it is relatively modest in comparison
574 with the natural range of variability. While our results suggest that the predicted increases
575 in burn rate *per se* will not move this ecosystem to new conditions never before
576 encountered in the past, the cumulative impacts of fire and clear-cutting or other low-
577 retention types of harvesting, which still prevail in this region, remain preoccupying. It
578 has already been shown that clear-cutting has considerably altered this system in terms of
579 age-class representation at the landscape level by diminishing the amount of stands
580 exceeding in age the length of the typical harvest rotation (Bergeron *et al.* 2006; Cyr *et*
581 *al*. 2009). An excessive use of even-aged management, therefore, contributes to eroding
582 the ecological resilience by reducing ecosystem variability in time and space (Drever *et*
583 *al*. 2006), a process that will be exacerbated by the predicted increase in burn rate.
584
585 **Acknowledgements**
586 We thank M. Jianguo Huang for his helpful comments on the manuscript and Isabelle
587 Lamarre for linguistic revision. This project was financially supported by the Natural
588 Sciences and Engineering Research Council of Canada (NSERC; Strategic project) and
589 the Canada Chair in Forest Ecology and Management to Dr. Yves Bergeron at the
590 Université du Québec en Abitibi-Témiscamingue, Canada.
591

Authors' contributions

The work presented here was carried out in collaboration between all authors. Y. Bergeron initiated the project and the initial draft of the manuscript. D. Cyr and C. Carcaillet provided and analyzed the sedimentary charcoal data, and interpreted the results. M.P. Girardin carried out the work with the GCM experiments, analyzed the data and interpreted the results. All authors have contributed to, seen and approved the manuscript.

References

Ali AA, Asselin H, Larouche AC, Bergeron Y, Carcaillet C, Richard PJH (2008) Changes in fire regime explain the Holocene rise and fall of *Abies balsamea* in the coniferous forests of western Québec, Canada. *The Holocene* **18**, 693–703.

Ali AA, Carcaillet C, Bergeron Y (2009) Long-term fire frequency variability in the eastern Canadian boreal forest: the influences of climate vs. local factors. *Global Change Biology* **15**, 1230-1241.

Angelstam PK (1998) Maintaining and restoring biodiversity in European boreal forests by developing natural disturbance regimes. *Journal of Vegetation Science* **9**, 593–602.

Attiwill PM (1994) The disturbance of forest ecosystems: The ecological basis for conservative management. *Forest Ecology and Management* **63**, 247–300.

616

617 Balshi MS, McGuire AD, Duffy P, Flannigan M, Walsh J, Melillo J (2009) Assessing the
618 response of area burned to changing climate in western boreal North America using a
619 Multivariate Adaptive Regression Splines (MARS) approach. *Global Change Biology* **15**,
620 578–600. doi:10.1111/j.1365–2486.2008.01679.

621

622 Bergeron Y, Cyr D, Drever CR, Flannigan M, Gauthier S, Kneeshaw D, Lauzon È, Leduc
623 A, Le Goff H, Lesieur D, Logan K (2006) Past, current, and future fire frequencies in
624 Quebec's commercial forests: Implications for the cumulative effects of harvesting and
625 fire on age-class structure and natural disturbance-based management. *Canadian Journal*
626 *of Forest Research* **36**, 2737–2744.

627

628 Bergeron Y, Gauthier S, Flannigan M, Kafka V (2004) Fire regimes at the transition
629 between mixedwood and coniferous boreal forest in northwestern Quebec. *Ecology* **85**,
630 1916–1932.

631

632 Carcaillet C, Bergeron Y, Richard PJH, Fréchette B, Gauthier S, Prairie YT (2001)
633 Change of fire frequency in the eastern Canadian boreal forests during the Holocene:
634 Does vegetation composition or climate trigger the fire regime? *Journal of Ecology* **89**,
635 930–946.

636

637 Carcaillet C, Richard PJH, Bergeron Y, Fréchette B, Ali AA (accepted) Resilience of the
638 boreal forest in response to fire-frequency changes during the Holocene assessed by
639 pollen diversity and population dynamics. *International Journal of Wildland Fire*
640
641 Chambers SD, Chapin FS III (2002) Fire effects on surface-atmosphere energy exchange
642 in Alaskan black spruce ecosystems: implications for feedbacks to regional climate.
643 *Journal of Geophysical Research* **107.** doi:10.1029/2001JD000530.
644
645 Cyr D, Gauthier S, Bergeron Y, Carcaillet C (2009) Forest management is driving the
646 eastern North American boreal forest outside its natural range of variability. *Frontiers in*
647 *Ecology and the Environment* **9** doi:10.1890/080088.
648
649 Dale VH, Joyce LA, McNulty S, Neilson RP, Ayres MP, Flannigan MD, Hanson PJ,
650 Irland LC, Lugo AE, Peterson CJ, Simberloff D, Swanson FJ, Stocks BJ, Wotton BM
651 (2001) Climate change and forest disturbances. *Bioscience* **51,** 723–734.
652
653 de Groot, WJ, Bothwell PM, Carlsson DH, Logan KA (2003) Simulating the effects of
654 future fire regimes on western Canadian boreal forests. *Journal of Vegetation Science* **14**,
655 355–364.
656
657 de Groot WJ, Pritchard JM, Lynham TJ (2009) Forest floor fuel consumption and carbon
658 emissions in Canadian boreal forest fires. Canadian Journal of Forest Research 39, 367–
659 382.
660

661 Drever CR, Peterson G, Messier C, Bergeron Y, Flannigan M (2006) Can forest
662 management based on natural disturbances maintain ecological resilience? *Canadian*
663 *Journal of Forest Research* **36**, 2285–2299.
664
665 Environment Canada (2006) Canadian climate normals or averages 1971–2000. Canadian
666 Climate Program, Environment Canada, Atmospheric Environment Service, Downsview,
667 Ontario, Canada. Available at
668 http://climate.weatheroffice.ec.gc.ca/climate_normals/index_f.html
669
670 Flannigan MD, Krawchuk MA, de Groot WJ, Wotton, BM, Gowman LM (2009)
671 Implications of changing climate for global wildland fire. *International Journal of*
672 *Wildland Fire* **18**, 483–507.
673
674 Friedman JH (1991) Multivariate adaptive regression splines. *Annals of Statistics* **19**, 1–
675 67.
676
677 Garralla S, Gajewski K (1992) Holocene vegetation history of the boreal forest near
678 Chibougamau, central Quebec. *Canadian Journal of Botany* **70**, 1364-1368.
679
680 Gauthier S, De Grandpré L, Bergeron Y (2000) Differences in forest composition in two
681 boreal forest ecoregions of Quebec. *Journal of Vegetation Science* **11**, 781–790.
682

683 Gauthier S, Vaillancourt M-A, Leduc A, De Grandpré L, Kneeshaw D, Morin H, Drapeau
684 P, Bergeron Y (2009) Ecosystem management in the boreal forest. (Les Presses de
685 l'Université du Québec: Quebec, Canada)
686
687 Gillett NP, Weaver AJ, Zwiers FW, Flannigan MD (2004) Detecting the effect of climate
688 change on Canadian forest fires. *Geophysical Research Letters* **31**, L18211. doi:10.1029-
689 2004GL0.0876.
690
691 Girardin M-P, Tardif J, Flannigan MD, Wotton BM, Bergeron Y (2004) Trends and
692 periodicities in the Canadian Drought Code and their relationships with atmospheric
693 circulation for the southern Canadian boreal forest. *Canadian Journal of Forest Research*
694 **34**, 103–119.
695
696 Girardin MP, Mudelsee M (2008) Past and future changes in Canadian boreal wildfire
697 activity. *Ecological Applications* **18(2)**, 391–406.
698
699 Girardin MP, Wotton BM (2009) Summer moisture and wildfire risks across Canada.
700 *Journal of Applied Meteorology and Climatology* **48**, 517–533.
701
702 Girardin MP, Ali AA, Carcaillet C, Mudelsee M, Drobyshev I, Hély C, Bergeron Y
703 (2009a) Heterogeneous response of circumboreal wildfire risk to climate change since the
704 early 1900s. *Global Change Biology* **15**, 2751-2769.
705

706 Girardin MP, Tardif JC, Epp B, Conciatori F (2009b) Frequency of cool summers in
707 interior North America over the past three centuries. *Geophysical Research Letters* **36**,
708 L07705. doi:10.1029/2009GL037242.
709
710 Harvey BD, Leduc A, Gauthier S, Bergeron Y (2002) Stand-landscape integration in
711 natural disturbance-based management of the southern boreal forest. *Forest Ecology and*
712 *Management* **155**, 369–385.
713
714 Hély C, Flannigan M, Bergeron Y, McRae D (2001) Role of vegetation and weather on
715 fire behavior in the Canadian mixedwood boreal forest using two fire behavior prediction
716 systems. *Canadian Journal of Forest Research* **31**, 430–441.
717
718
719 Higuera PE, Peters ME, Brubaker LB, Gavin DG (2007) Understanding the origin and
720 analysis of sediment charcoal records with a simulation model. *Quaternary Science*
721 *Reviews **26***, 1790–1809.
722
723 Intergovernmental Panel on Climate Change (2007) General guidelines on the use of
724 scenario data for climate impact and adaptation assessment (version 2). Task Group on
725 Data and Scenario Support for Impact and Climate Assessment (TGICA). Finnish
726 Environment Institute, Helsinki, Finland.
727

728 Jasinski JPP, Payette S (2005) The creation of alternative stable states in the southern
729 boreal forest, Québec, Canada. *Ecological Monographs* **75**, 561–583.
730
731 Keane RE, Cary GJ, Davies ID, Flannigan MD, Gardner RH, Lavorel S, Lenihan JM, Li
732 C, Rupp TS (2004) A classification of landscape fire succession models: spatial
733 simulations of fire and vegetation dynamics. *Ecological Modelling* **179**, 3–27.
734
735 Kuuluvainen T (2002) Natural variability of forests as a reference for restoring and
736 managing biological diversity in boreal Fennoscandia. *Silva Fennica* **36**, 97–125.
737
738 Landres PB, Morgan P, Swanson FJ (1999) Overview of the use of natural variability
739 concepts in managing ecological systems. *Ecological Applications* **9**, 1179–1188.
740
741 Leathwick JR, Rowe D, Richardson J, Elith J, Hastie T (2005) Using multivariate
742 adaptive regression splines to predict the distributions of New Zealand's freshwater
743 diadromous fish. *Freshwater Biology* **50**, 2034–2052.
744
745 Lecomte N, Bergeron Y (2005) Successional pathways on different surficial deposits in
746 the coniferous boreal forest of the Quebec Clay Belt. *Canadian Journal of Forest*
747 *Research* **35**, 1984–1995.
748

749 Lecomte N, Simard M, Fenton N, Bergeron Y (2006) Fire severity and long-term
750 ecosystem biomass dynamics in coniferous boreal forests of eastern Canada. *Ecosystems*
751 **9**, 1215–1230.
752
753 Lefort P, Gauthier S, Bergeron Y (2003) The influence of fire weather and land use on
754 the fire activity of the Lake Abitibi area, Eastern Canada. *Forest Science* **49**, 509–521.
755
756 Le Goff H, Leduc A, Bergeron Y, Flannigan M (2005) The adaptative capacity of forest
757 management to changing fire regimes in the boreal forest of Quebec. *The Forestry*
758 *Chronicle* **81**, 582–592.
759
760 Li, C. 2002. Estimation of fire frequency and fire cycle: A computational perspective.
761 Ecological Modelling **154,** 103-120.
762
763 Li C, Flannigan MD, Corns IGW (2000) Influence of potential climate change on forest
764 landscape dynamics of west-central Alberta. *Canadian Journal of Forest Research* **30**,
765 1905–1912.
766
767 McAlpine RS (1990) Seasonal trends in the Drought Code component of the Canadian
768 Forest Fire Weather Index System. Forestry Canada, Petawawa National Forestry
769 Institute, Chalk River, ON, Canada, Information Report PI-X-97 E/F. (Chalk River, ON).
770

771 Macias-Fauria M, Johnson EA (2006) Large-scale climatic patterns control large
772 lightning fire occurrence in Canada and Alaska forest regions. *Journal of Geophysical*
773 *Research* **111**, G04008. doi:10.1029/2006JG000181.
774
775 Martell DL (1994) The impact of fire on timber supply in Ontario. *The Forestry*
776 *Chronicle* **70**, 164–173.
777
778 Meehl GA, Stocker TF, Collins WD, Friedlingstein P, Gaye AT, Gregory JM, Kitoh A,
779 Knutti R, Murphy JM, Noda A, Raper SCB, Watterson IG, Weaver AJ, Zhao Z-C (2007)
780 'Global Climate Projections'. In: Climate Change 2007: The Physical Science Basis.
781 Contribution of Working Group I to the Fourth Assessment Report of the
782 Intergovernmental Panel on Climate Change. Solomon S, Qin D, Manning M, Chen Z,
783 Marquis M, Averyt KB, Tignor M, Miller HL (eds.). (Cambridge University Press:
784 Cambridge, New York, NY).
785
786 Merril, D.F., and Alexander, M.E. (eds). (1987) Glossary of forest fire management
787 terms. National Research Counsil of Canada, Canadian Committee on Forest Fire
788 management. Publication No. 25616, Ottawa.
789
790 Nakicenovic N, *et al.* (2000) IPCC Special Report on Emission Scenarios. (Cambridge
791 University Press: Cambridge, UK).
792

793 Niklasson M, Granström, Anders (2000) Numbers and sizes of fires: Long-term spatially
794 explicit fire history in a Swedish boreal landscape. *Ecology* **81**, 1484-1499.
795
796 Overpeck JT, Rind D, Goldberg R (1990) Climate-induced changes in forest disturbance
797 and vegetation. *Nature* **343**, 51-53.
798
799 Podur J, Martell DL, Knight K (2002) Statistical quality control analysis of forest fire
800 activity in Canada. *Canadian Journal of Forest Research* **32**, 195–205.
801
802 Price C, Rind D (1994) The impact of a $2 \times CO_2$ climate on lightning-caused fires.
803 *Journal of Climate* **7**, 1484–1494.
804
805 Régnière J, Bolstad P (1994) Statistical simulation of daily air temperature patterns in
806 eastern North America to forecast seasonal events in insect pest management.
807 *Environmental Entomology* **23**, 1368–1380.
808
809 Reynolds CS (2002) Ecological pattern and ecosystem theory. *Ecological Modelling* **158**,
810 181–200.
811
812 R Development Core Team (2007) 'R: a language and environment for statistical
813 computing'. (R Foundation for Statistical Computing. Vienna, Austria). http://www.R-
814 project.org.

815 Scholze M, KnorrW, Arnell NW, Prentice IC (2006) A climate-change risk analysis for
816 world ecosystems. *Proceedings of the National Academy of Sciences of the United States*
817 *of America* **103**, 13 116–13 120. doi:10.1073/PNAS.0601816103
818
819 Skinner WR, Shabbar A, Flannigan MD, Logan K (2006) Large forest fires in Canada
820 and the relationship to global sea surface temperatures. *Journal of Geophysical Research*
821 **111**, D14106. doi:10.1029/2005JD006738.
822
823 Soil Classification Working Group (1998) 'The Canadian System of Soil Classification.
824 3rd edition'. (Agriculture and Agri-Food Canada, Ottawa, ON).
825
826 Stocks BJ, Mason JA, Todd JB, Bosch EM, Wotton BM, Amiro BD, Flannigan MD,
827 Hirsch KG, Logan KA, Martell DL, Skinner WR (2003) Large forest fires in Canada,
828 1959-1997. *Journal of Geophysical Research* **107**, 8149. doi:10.1029/2001JD000484.
829
830 Thornthwaite CW, Mather JR (1955) The water balance. *Publications in Climatology* **8**,
831 1–86.
832
833 United Nations (1992) United Nations Framework Convention on Climate Change.
834 FCCC/INFORMAL/84, GE.05-62220 (E) 200705.
835 http://unfccc.int/resource/docs/convkp/conveng.pdf (last accessed January 27, 2010).
836

837 Van Wagner CE (1987) Development and structure of the Canadian Forest Fire Weather
838 Index System. Canadian Forestry Service, Petawawa National Forestry Institute, Forestry
839 Technical Report 35. (Chalk River, ON).
840
841 Veillette JJ (1994) Evolution and paleohydrology of glacial Lakes Barlow and Ojibway.
842 *Quaternary Science Reviews* **13**, 945–971.
843
844 Weber MG, Flannigan MD (1997) Canadian boreal forest ecosystem structure and
845 function in a changing climate: impact on fire regimes. *Environmental Reviews* **5**, 145–
846 166.
847
848 Wotton BM, Martell DL, Logan KA (2003) Climate change and people-caused forest fire
849 occurrence in Ontario. *Climatic Change* **60**, 275–295.

850

851 **Table 1**. General circulation models from the Intergovernmental Panel on Climate

852 Change Fourth Assessment Report (AR4; Meehl *et al.* 2007) and their greenhouse gas

853 (e.g. radiative) forcing scenarios.

Centre	**Model**	**Forcing**
Bjerknes Centre for Climate	BCM2.0	A1B, A2, B1
Canadian Centre for Climate Modelling and Analysis (CCCma)	CGCM3T63 (T63 resolution)	A1B, A2, B1
Australia's Commonwealth Scientific and Industrial Research Organisation (CSIRO)	CSIROMk3.5	A1B, A2, B1
Max Planck Institute für Meteorologie	ECHAM4T42	A2, B2
GISS	GISSAOM	A1B, B1
Institute for Numerical Mathematics	INMCM3.0	A1B, A2, B1
National Institute for Environmental Studies	MIROC3.2 medres	A1B, A2, B1

854

855 **Table 2**. Predicted burn rates (% yr^{-1}) from ensemble-mean scenarios for horizons

856 1961–1999, 2046–2065, and 2081–2100. Each ensemble simulation shown here consists

857 of an average of six general circulation model experiments undertaken with identical

858 forcing scenarios (A2, A1B, and B1). A 95% bootstrap confidence interval (CI) for the

859 ensemble-mean burn rate is indicated in brackets.

	Scenario		
	A2	A1B	B1
GCM[a]	BCM2.0, CGCM3T63, CSIROMk3.5, ECHAM4T42, INMCM3.0, MIROC3.2 medres	BCM2.0, CGCM3T63, CSIROMk3.5, GISSAOM, INMCM3.0, MIROC3.2 medres	BCM2.0, CGCM3T63, CSIROMk3.5, GISSAOM, INMCM3.0, MIROC3.2 medres
1961-1999	0.22 [0.10; 0.36]	0.22 [0.09; 0.35]	0.22 [0.09; 0.35]
2046-2065	0.40 [0.21; 0.61]	0.37 [0.22; 0.54]	0.29 [0.13; 0.47]
2081-2100	0.55 [0.33; 0.80]	0.42 [0.21; 0.63]	0.35 [0.19; 0.53]

860 a GCMs used in each climate change scenario.

861

862

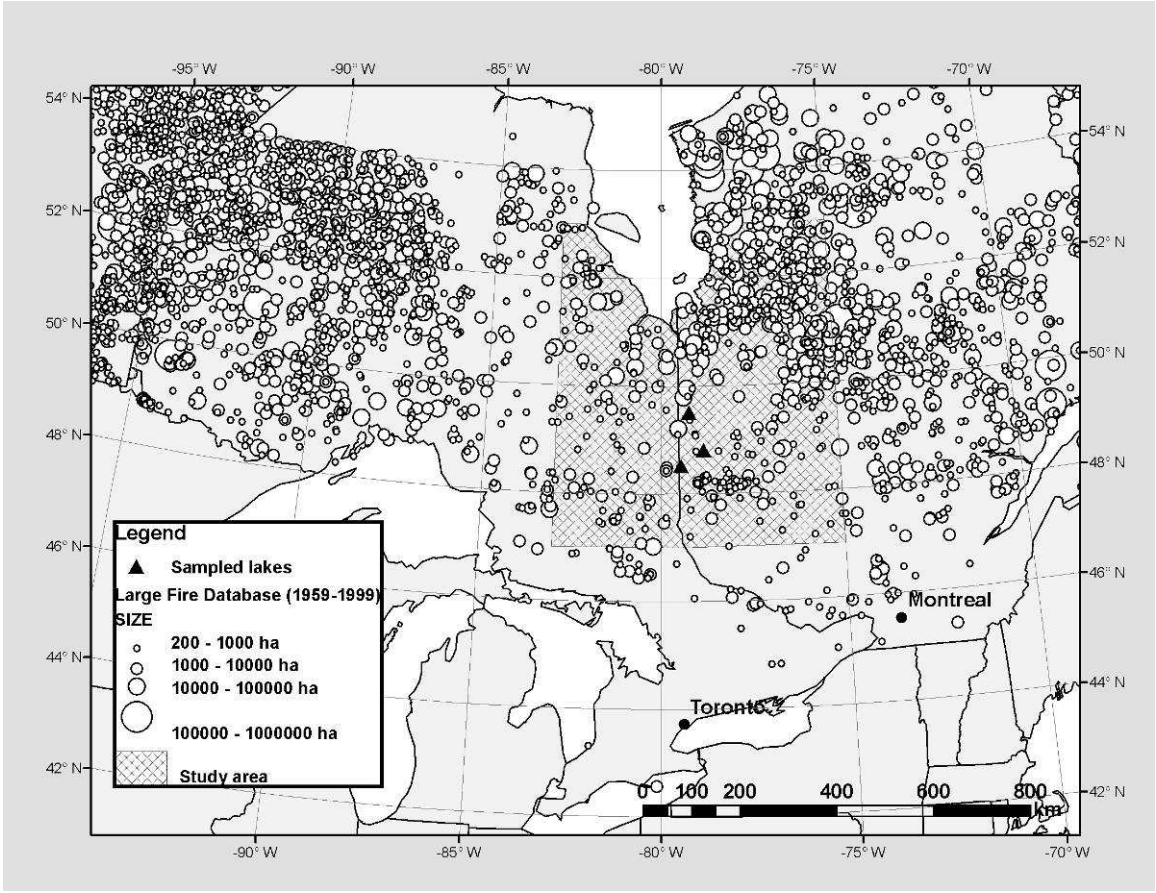

Fig. 1. Location of the three lakes for which sedimentary charcoal analyses were conducted. The study area (shaded) delineates forest fire data (circles) from the large fire database (LFDB, Stocks *et al*. 2003) that were used in this study to develop the annual area burned model.

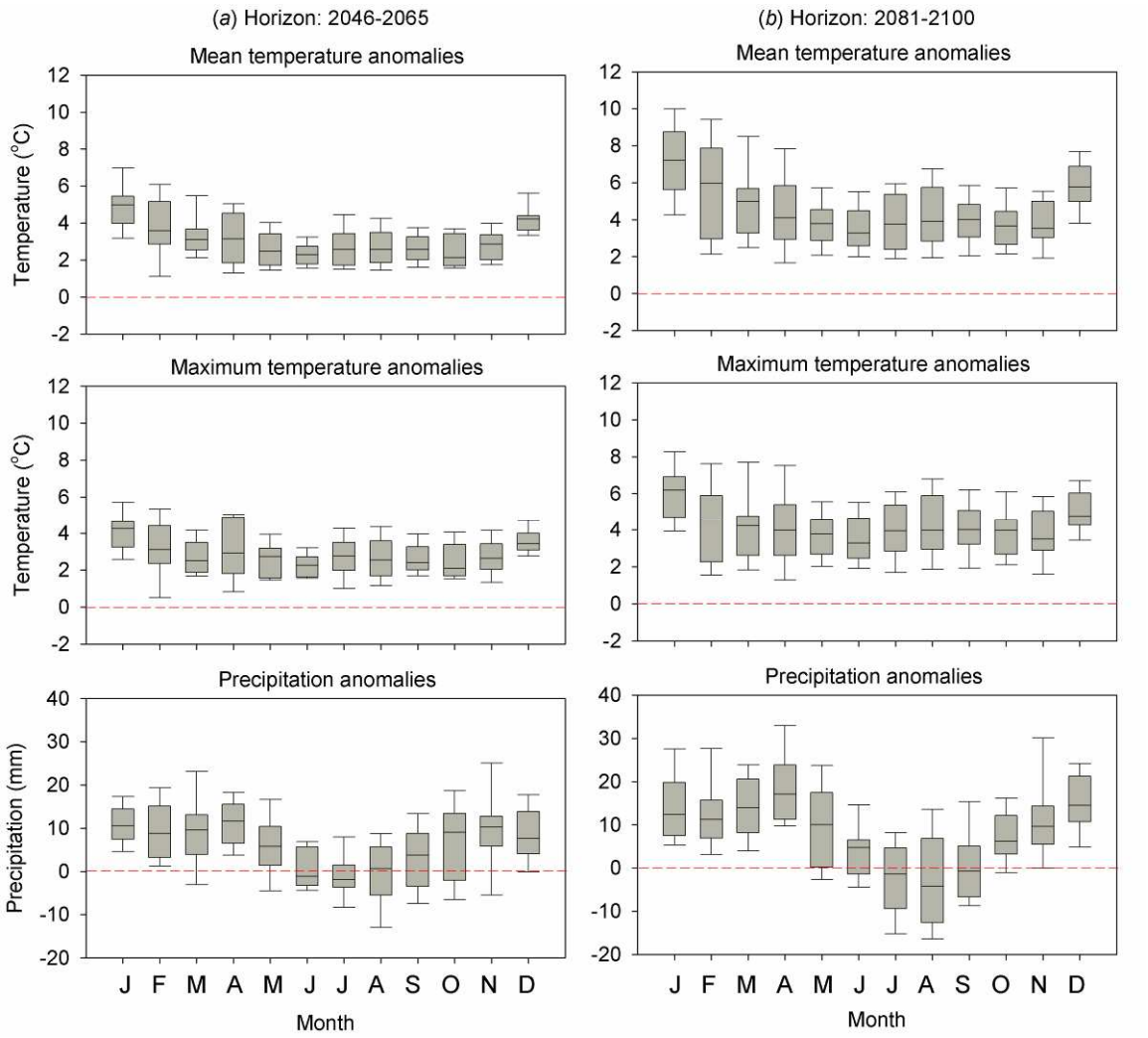

Fig. 2. Predicted changes in monthly averages of daily mean and daily maximum temperatures, and total monthly precipitation between a) 2046–2065 and 1961–1999, and b) 2081–2100 and 1961–1999. Simulations were obtained using an ensemble-mean of seven global climate models forced by various scenarios of greenhouse gas emissions (Table 1), for a total of 19 simulations. The boxplot shows the distribution of the 19 simulation results for January (J) to December (D). The boundaries of the box denote the 25th and 75th percentiles, and the line within the box marks the median of the simulated mean monthly anomalies. Error bars above and below the box indicate the 90th and 10th percentiles.

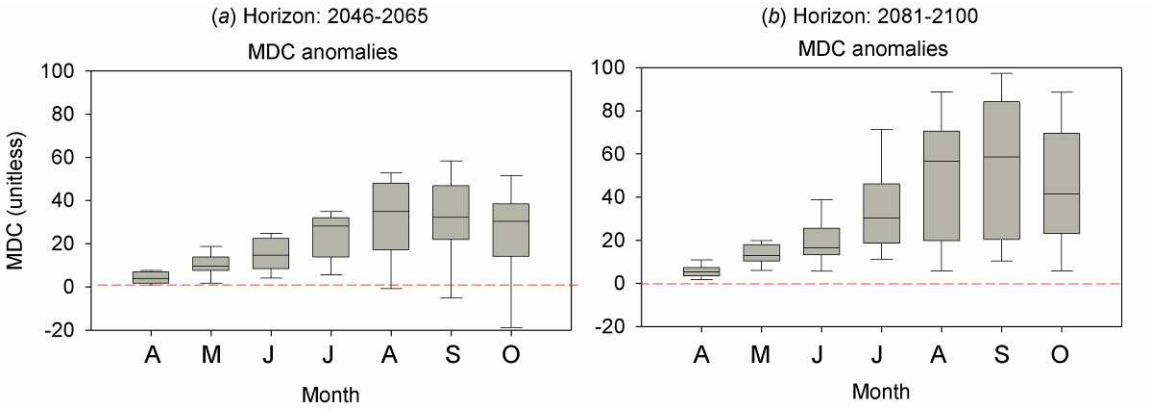

1

2 **Fig. 3.** Predicted changes in monthly Drought Code (MDC) between a) 2046–2065 and

3 1961–1999, and b) 2081–2100 and 1961–1999. See Fig. 2 for definition.

4

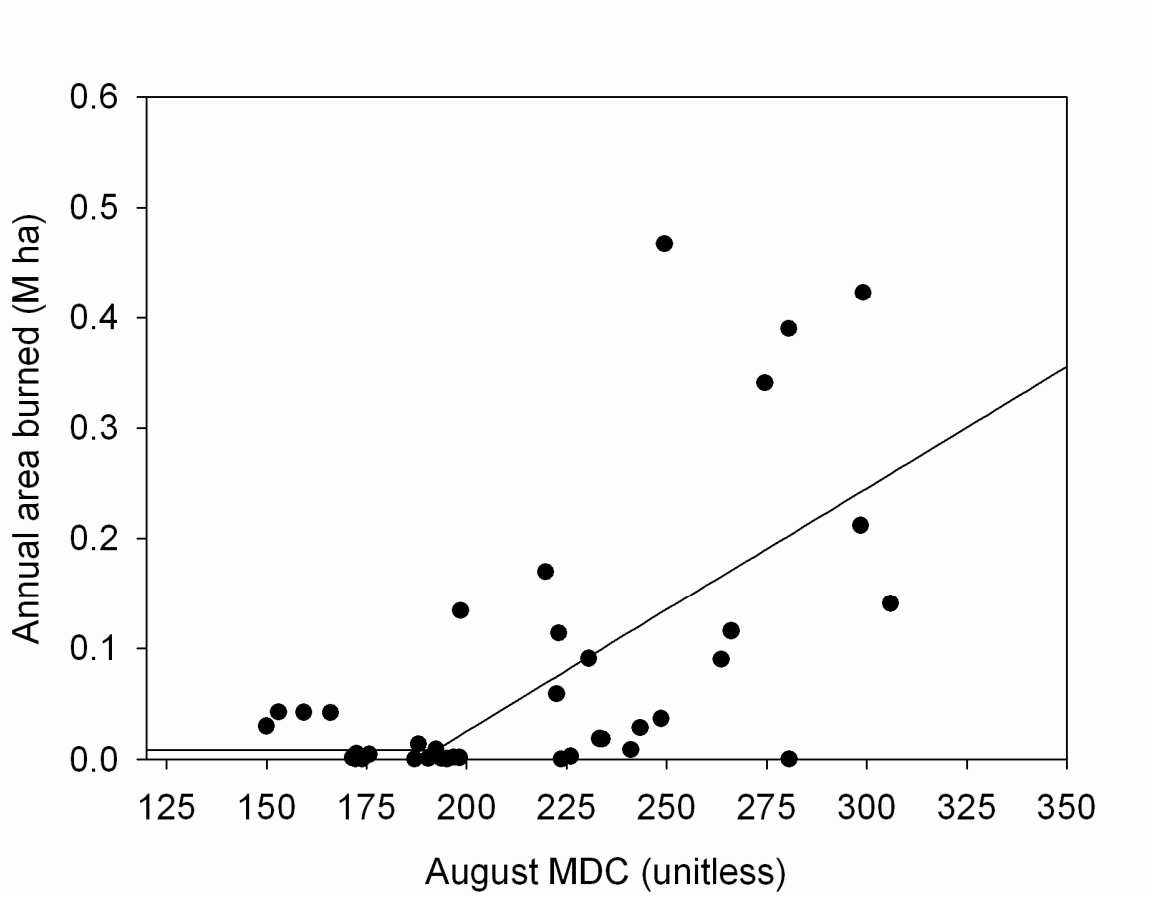

Fig. 4. Relationships between the August monthly Drought Code (MDC) and annual area burned (AAB) modeled using Multivariate Adaptive Regression Splines.

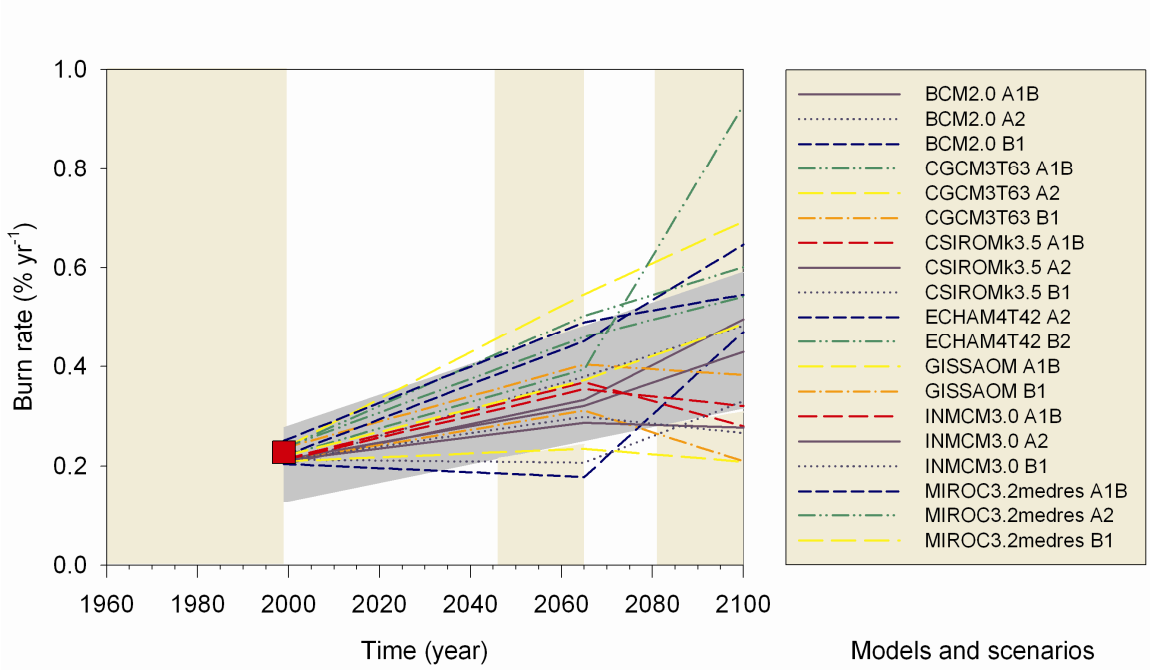

Fig. 5. Predicted changes in burn rate over the 21st century simulated from an ensemble of seven global climate models forced by various scenarios of greenhouse gas emissions (Table 1). A 95% bootstrap confidence interval for the ensemble-mean burn rate is shown (gray-shaded). The latter was obtained after randomization of the annual area burned (AAB) simulations and recomputation of the burn rate for each horizon using the upper and lower AAB percentiles. The yellow shading denotes the three horizons (1961–1999, 2046–2065, and 2081–2100) used in the computation of the future burn rate. See Table 2 for individual ensemble-mean scenarios. The burn rate estimated from the LFDB is indicated by a red square

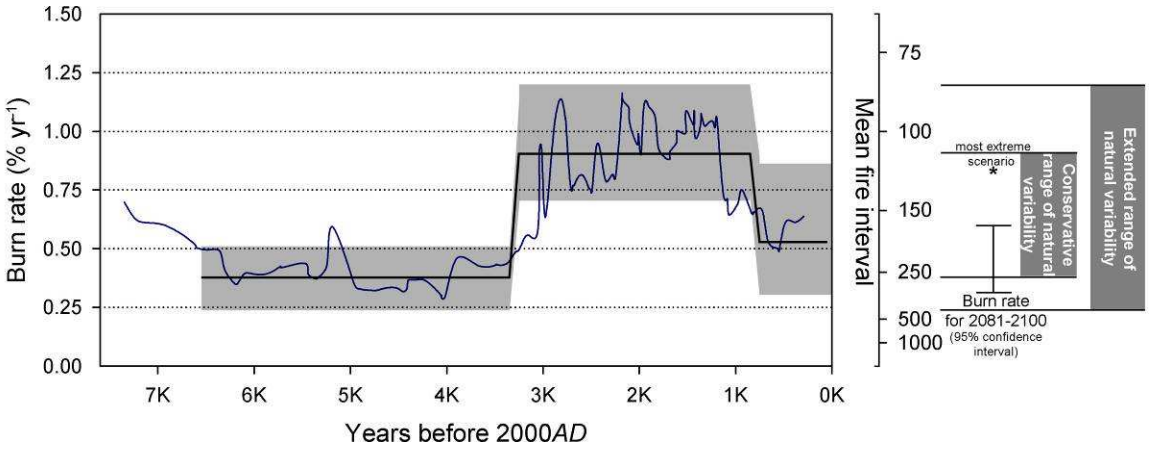

Fig. 6. Long-term variability in burn rate compared with the burn rate for 2081-2100. Average burn rates during periods of relatively constant regime (straight lines) define the conservative range of natural variability, while the 95% confidence intervals (shaded area) define the extended range of natural variability. Shorter-term variations are illustrated for comparison purposes. Adapted from Cyr *et al*. 2009.